Journal of Hazardous Materials A107 (2004) 81–94

Journal of Hazardous Materials

www.elsevier.com/locate/jhazmat

The quantitative assessment of domino effect caused by overpressure Part II. Case studies

Valerio Cozzani [a], Ernesto Salzano [b,*]

[a] *Dipartimento di Ingegneria Chimica, Mineraria e delle Tecnologie Ambientali, Università di Bologna, viale Risorgimento 2, 40136 Bologna, Italy*
[b] *Istituto di Ricerche sulla Combustione, CNR, via Diocleziano 328, 80125 Napoli, Italy*

Received 8 July 2003; accepted 16 September 2003

Abstract

A quantitative assessment of the contribution to industrial risk of domino effect due to overpressure was undertaken by using the damage probability models developed in part I. Two case studies derived from the actual lay-out of an oil refinery were analyzed. Individual and societal risk indexes were estimated both in the absence and in the presence of the domino effects caused by overpressure. An increase of individual risk up to an order of magnitude was found when considering domino effects.

Keywords: Domino effect; Blast wave; Probit analysis; Quantitative risk analysis; Explosion

1. Introduction

Damage to equipment caused by blast waves is an important source of accidents involving domino effects [1–5]. Nevertheless, as discussed in part I [6], almost all the approaches reported in the literature are based on oversimplified methods for the estimation of the propagation probabilities, such as vulnerability tables or threshold values. Existing models for the assessment of the damage probability to the process equipment due to overpressure were revised in the part I, showing that they may lead to completely unrealistic propagation probability figures, with errors that not always are on the safe side. Hence, more detailed probit models were developed on the basis of available literature data for overpressure damage to the process equipment.

In the present study, a quantitative assessment of the contribution to industrial risk of domino effect due to overpressure was undertaken. Two case studies were defined, both derived from the actual lay-out of an existing oil refinery. Individual and societal risk indexes were then estimated in the presence and in the absence of domino effect using the Aripar-GIS 2.1 software [7]. The approach proposed by Cozzani and Zanelli [8] was used to assess the contribution of domino effect to the risk indexes. The probit models developed in part I, as well as other literature models were used to estimate damage probabilities of process equipment. The values of the risk indexes obtained from the different approaches were thus compared and analyzed.

2. The case studies

2.1. Definition of case studies and risk assessment not considering domino effect

The case studies were selected in order to allow the assessment of domino effects caused by overpressure between pressurized storage vessels, atmospheric process, or storage units. The choice was addressed by the analysis of historical records on domino events in the last decades [9,10], which evidenced that these units were the targets of some of the more severe domino events experienced. The case studies, described in detail in the following, were derived from the actual lay-out of an existing Italian oil refinery.

With respect to the consequence assessment of primary events (i.e. not considering domino effect) the guidelines proposed by the well-known “yellow book” and “purple book” [11,12] were followed for the definition of primary scenarios, for the selection of the expected frequencies, for the estimation of ignition probabilities, for the assessment

* Corresponding author. Tel.: +39-081-7621922; fax: +39-081-7622915.
E-mail address: salzano@irc.na.cnr.it (E. Salzano).

0304-3894/$ – see front matter © 2004 Elsevier B.V. All rights reserved.
doi:10.1016/j.jhazmat.2003.09.014

Nomenclature

EV	expectation value or potential life loss
f_D	frequency of the domino event
f_T	frequency of the primary top event
F	probability
F_d	probability of failure
F_e	probability of the secondary scenario, given the failure of the target unit
F_s	probability of the primary scenario
k_1	probit coefficient
k_2	probit coefficient
N	number of events
ΔP	static overpressure (kPa g)
ΔP_{th}	static overpressure, threshold (kPa g)
r_{th}	distance at which a threshold overpressure corresponding to 25% of probability of damage is reached (m)
V	vulnerabilities (death probabilities)
Y	probit

Subscript

°	peak

of pool fire radiation and in general for the assessment of the consequences of accidental events. For the estimation of societal risk, an homogeneous distribution of population was assumed, with a density of 5×10^{-3} workers/m^2. This approximation was necessary in order to obtain more comprehensible results, getting rid of discontinuities that may arise in societal risk results if an inhomogeneous population distribution is considered.

The Aripar-GIS 2.1 software was used to assess the individual and societal risk due to the accidental scenarios. The software as well as the methodology for the assessment of risk indexes is fully described elsewhere [7,13]. Starting from the well-known *F–N* curves representing the societal risk, the "expectation value" (EV) or potential life loss was also calculated [19]:

$$\mathrm{EV} = \int_0^N F(N)\,\mathrm{d}N \tag{1}$$

where N is the number of events.

The above risk indexes were calculated either not considering or taking into account of domino effect. In the context of the present study, only the domino effects caused by overpressure were analysed, whereas the potential domino hazard due to pool fire and jet fire radiation were not considered. Damage probabilities of process equipment due to overpressure were estimated by using both literature models and probit models developed in part I for the different categories of process equipment [6]. Table 1 summarizes the damage probability models. Besides the probit approach developed herein, damage probabilities were also calculated by using the Bagster and Pitblado model [14], the probit model proposed by Eisenberg et al. [15], and the approach proposed by Khan and Abbasi [16]. The latter consists of a probit model similar to that of Eisenberg et al. [15] jointly to a 70 kPa damage threshold. For the sake of comparison, the vulnerability model proposed by Gledhill and Lines [17], based on damage threshold values of 7 kPa for atmospheric equipment and of 38 kPa for pressurized vessels, was also considered. Extended discussion of the different damage probability models was presented in part I.

Table 1
Damage probability models

Model	Reference	Damage probability (F)	Equipment	Coefficients	
				k_1	k_2
Present study	[6]	$Y = k_1 + k_2 \ln(\Delta P^\circ)$, Y: probit for equipment failure; ΔP°: peak static overpressure (Pa)	Atmospheric	18.96	2.44
			Pressurized	42.44	4.33
			Elongated	28.07	3.16
			Small	−17.79	2.18
Bagster and Pitblado	[14]	$F_d = \left(1 - \frac{r}{r_{th}}\right)^2$, r: distance from explosion center (m); r_{th}: distance from explosion center at which static overpressure equals ΔP_{th}	All	$\Delta P_{th} = 36$ kPa	
Eisenberg et al.	[15]	$Y = k_1 + k_2 \ln(\Delta P^\circ) Y$, Y: probit for equipment failure; ΔP°: peak static overoverpressure (Pa)	All	−23.8	2.92
Khan and Abbasi	[16]	if $\Delta P^\circ < 70$ kPa : $F_d = 0$ if $\Delta P^\circ \geq 70$ kPa : $Y = k_1 + k_2 \ln(\Delta P^\circ) Y$: probit for equipment failure; ΔP°: sum of static and dynamic overpressure (kPa)	All	−23.8	2.92
Gledhill and Lines	[17]	if $\Delta P^\circ < \Delta P_{th}$: $F_d = 0$ if $\Delta P^\circ \geq \Delta P_{th}$: $F_d = 1$	Atmospheric Pressurized	$\Delta P_{th} = 7$ kPa $\Delta P_{th} = 38$ kPa	

F_d: failure probability; Y: probit value corresponding to failure probability.

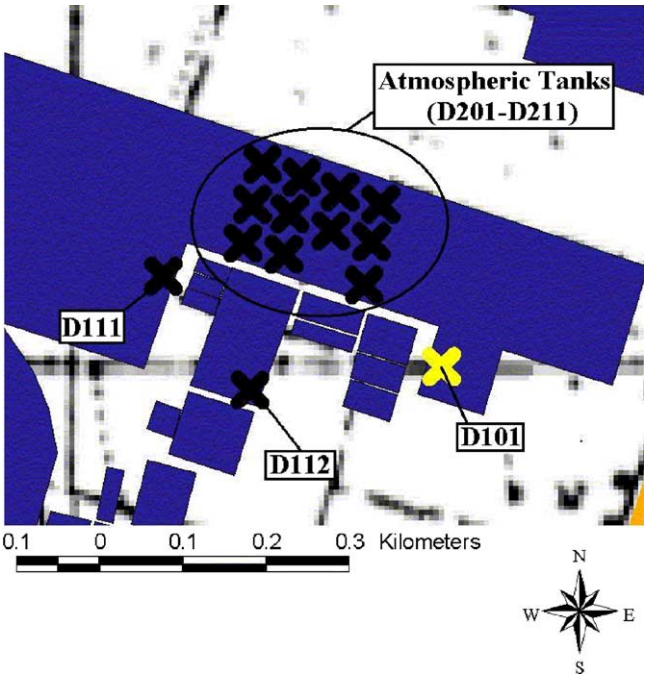

Fig. 1. Lay-out defined for case study 1.

2.2. Case study 1: LPG storage vessels and atmospheric tank farm

Case study 1 refers to the quantitative risk assessment of two adjacent storage units: a storage area for atmospheric fuel tanks and an LPG tank farm. Fig. 1 reports the lay-out considered in the analysis. The atmospheric tank farm is composed of 11 atmospheric storage tanks, each storing 8000 t of low volatility fuel oil. The LPG storage was schematized as composed of three pressurized vessels: a 1000 t butane sphere and two horizontal pressurized storage tanks containing propane. Table 2 reports a complete list of the equipment and the inventory. Layout data are completed by Table 3, which reports the distances between the LPG vessels and the atmospheric tanks.

Table 2
Storage vessels of atmospheric storage unit and of the nearby LPG farm as considered for case 1

Vessel	Type	Substance	Content, t
D101	Pressurized tank	Butane	1000
D111	Pressurized tank	Propane	50
D112	Pressurized tank	Propane	50
D201	Atmospheric tank	Fuel oil	8000
D202	Atmospheric tank	Fuel oil	8000
D203	Atmospheric tank	Fuel oil	8000
D204	Atmospheric tank	Fuel oil	8000
D205	Atmospheric tank	Fuel oil	8000
D206	Atmospheric tank	Fuel oil	8000
D207	Atmospheric tank	Fuel oil	8000
D208	Atmospheric tank	Fuel oil	8000
D209	Atmospheric tank	Fuel oil	8000
D210	Atmospheric tank	Fuel oil	8000
D211	Atmospheric tank	Fuel oil	8000

Table 3
Distances between equipment and calculated peak overpressures (ΔP°, kPa) for case study 1

	Distance (m)			ΔP° (kPa)		
	D101	D111	D112	D101	D111	D112
D101	–	355	242	–	11	20
D111	355	–	171	38	–	38
D112	242	171	–	69	38	–
D201	326	184	274	42	32	17
D202	282	207	265	54	26	18
D203	244	235	264	72	22	18
D204	209	280	275	92	17	17
D205	300	142	225	47	50	23
D206	264	174	219	62	35	25
D207	211	209	218	91	26	25
D208	174	258	233	100	19	22
D209	133	242	188	100	20	31
D210	282	106	181	53	85	33
D211	232	146	170	75	48	36

The primary scenarios considered for the risk assessment of this case study are reported in Table 4. It is worth noting that the primary scenarios considered were limited to pool fires for the atmospheric tank, since the low volatility of fuel oil limits the formation of flammable clouds due to pool vaporization. With respect to the LPG vessels, a reduced set of primary scenarios has been considered for the sake of simplicity. Fig. 2 shows the calculated peak overpressure with respect to distance for the UVCEs considered as primary accidental scenarios. Figs. 3 and 4 show the individual and societal risk calculated for the case study 1, without considering domino effect. These results will be used in the following to understand the contribution of domino effect to the risk indexes.

The UVCEs considered in the consequence analysis were considered as possible sources of domino effect. On the basis of the blast curves reported in Fig. 2, the resulting overpressures on the adjacent equipment were evaluated.

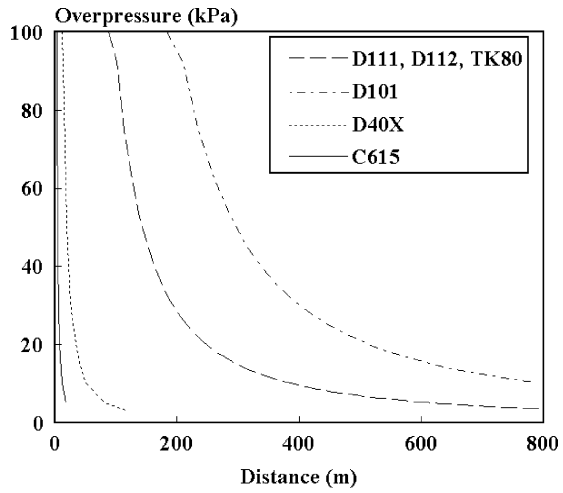

Fig. 2. Overpressures as a functions of distance for the primary UVCEs considered in the two case studies.

Table 4
Primary scenarios considered for the two case studies

Case study	Vessel	Top event	Frequency, events/year	Scenario	Probability
1	D101 (LPG sphere)	Leak (10 mm)	1×10^{-5}	Jet fire	0.20
				Flash fire	0.50
		Instantaneous release (complete content)	1×10^{-6}	Fire ball	0.70
				Flash fire	0.12
				UVCE	0.08
	D111 and D112 (LPG horizontal storage vessels)	Leak (10 mm)	1×10^{-5}	Jet fire	0.20
				Flash fire	0.50
		Instantaneous release (complete content)	1×10^{-6}	Fire ball	0.70
				Flash fire	0.12
				UVCE	0.08
	D201–D211 (atmospheric storages)	Leak (10 mm)	1×10^{-4}	Pool fire	0.10
		Instantaneous release	1×10^{-5}	Pool fire	0.10
2	C615 (distillation column)	Leak (10 mm)	1×10^{-4}	Pool fire	0.10
				Flash fire	0.50
		Instantaneous release (complete content)	1×10^{-5}	Pool fire	0.10
				Flash fire	0.30
				UVCE	0.20
	TK80 (LPG horizontal storage vessels)	Leak (10 mm)	1×10^{-5}	Jet fire	0.20
				Flash fire	0.50
		Instantaneous release (complete content)	1×10^{-6}	Fire ball	0.70
				Flash fire	0.12
				UVCE	0.08
	D401–408 (atmospheric storages)	Leak (10 mm)	1×10^{-4}	Pool fire	0.10
		Instantaneous release (complete content)	1×10^{-5}	Pool fire	0.10
				Flash fire	0.30
				UVCE	0.20

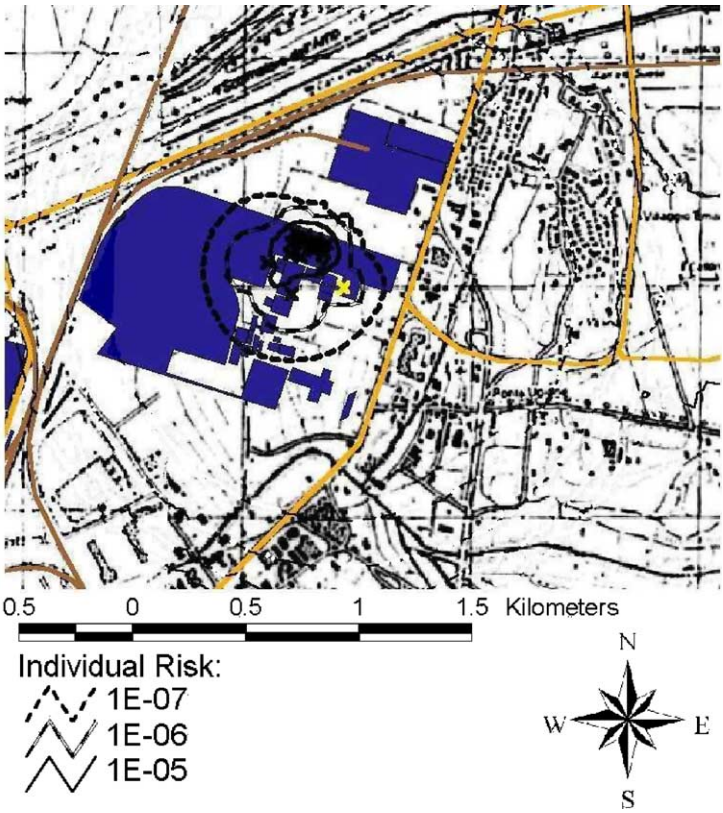

Fig. 3. Individual risk in the absence of domino effect for case study 1.

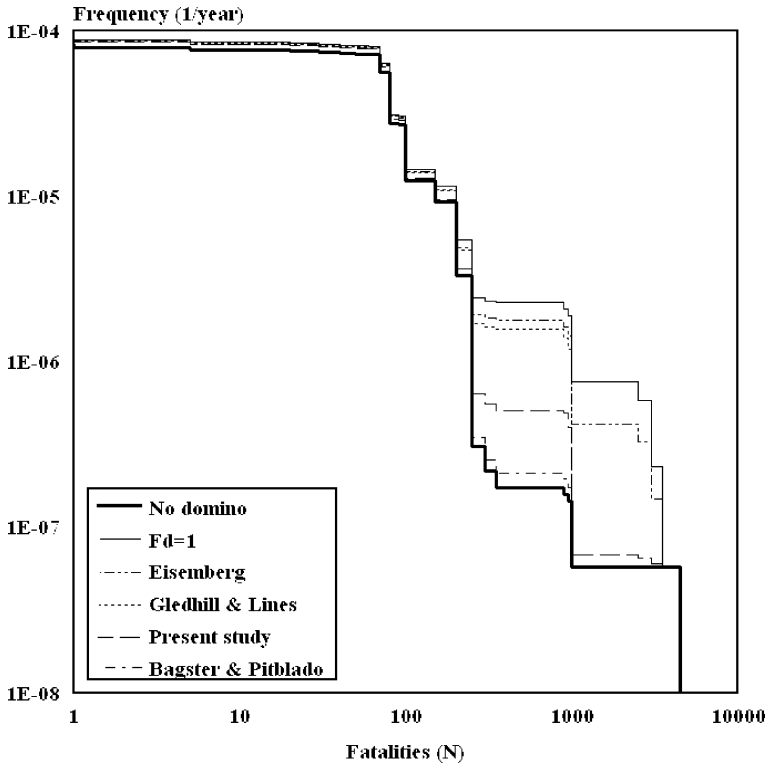

Fig. 4. Societal risk (*F–N* curves) calculated for case study 1.

Table 3 shows the results obtained. The explosion center was assumed at the location of the specific storage vessel involved in the accidental release of the liquid fuel, also considered as the center of the vapour cloud.

Table 5 shows the damage probabilities calculated for each vessel considered in the case study 1 on the basis of the distance from explosion center and vessel category. As expected, the high overpressures caused by the severe primary accidents considered in the simulation (UVCEs following a catastrophic vessel rupture) were found to cause very high damage probabilities on the atmospheric storage vessels. Damage probabilities close to one (damage is certain) are obtained for almost all the atmospheric vessels either using the probit model, developed in the present study, or the model by Eisenberg et al. [15]. On the other hand, the 70 kPa threshold value used in the approach of Khan and Abbasi [16] is seldom exceeded, and a zero damage probability results in this approach for most of the atmospheric vessels. It must be also remarked that, when the 70 kPa threshold is reached, the probit model given by Khan and Abbasi yields a damage probability near to one (damage is certain).

Table 5
Damage probabilities calculated by using different damage propagation models for case study 1

	Present study			Bagster and Pitblado [14]			Khan and Abbasi [16]			Eisenberg et al. [15]			Gledhill and Lines [17]		
	D101	D111	D112	D101	D111	D112	D111	D112	D112	D101	D111	D112	D101	D111	D112
D101	–	0.00	0.00	–	0.00	0.00	–	0.00	0.00	–	0.07	0.55	–	0.00	0.00
D111	0.03	–	0.03	0.00	–	0.00	0.00	–	0.00	0.96	–	0.96	1.00	–	1.00
D112	0.79	0.03	–	0.11	0.00	–	0.00	0.00	–	1.00	0.96	–	1.00	1.00	–
D201	0.97	0.91	0.49	0.01	0.00	0.00	0.00	0.00	0.00	0.99	0.90	0.42	1.00	1.00	1.00
D202	1.00	0.80	0.52	0.05	0.00	0.00	0.00	0.00	0.00	1.00	0.81	0.45	1.00	1.00	1.00
D203	1.00	0.68	0.52	0.11	0.00	0.00	1.00	0.00	0.00	1.00	0.66	0.45	1.00	1.00	1.00
D204	1.00	0.40	0.49	0.18	0.00	0.00	1.00	0.00	0.00	1.00	0.30	0.42	1.00	1.00	1.00
D205	0.99	1.00	0.73	0.03	0.04	0.00	0.00	0.00	0.00	1.00	1.00	0.70	1.00	1.00	1.00
D206	1.00	0.95	0.77	0.07	0.00	0.00	0.00	0.00	0.00	1.00	0.96	0.76	1.00	1.00	1.00
D207	1.00	0.80	0.77	0.17	0.00	0.00	1.00	0.00	0.00	1.00	0.81	0.76	1.00	1.00	1.00
D208	1.00	0.53	0.69	0.27	0.00	0.00	1.00	0.00	0.00	1.00	0.47	0.66	1.00	1.00	1.00
D209	1.00	0.60	0.90	0.40	0.00	0.00	1.00	0.00	0.00	1.00	0.55	0.88	1.00	1.00	1.00
D210	1.00	1.00	0.93	0.05	0.16	0.00	0.00	1.00	0.00	1.00	1.00	0.92	1.00	1.00	1.00
D211	1.00	1.00	0.95	0.13	0.03	0.00	1.00	0.00	0.00	1.00	1.00	0.96	1.00	1.00	1.00

The Bagster and Pitblado [14] model, based on a damage threshold of 36 kPa, yields a damage threshold distance r_{th} of 364 m for the UVCE caused by the butane sphere D101, and a damage threshold distance of 175 m for the propane vessels D111 and D112. Thus, damage probabilities caused by the primary UVCEs originated from vessels D111 and D112, if present, result very low, while those caused by the UVCE originated from vessel D101 are consistent. The analysis of Tables 3 and 5 also shows that the Bagster and Pitblado [14] model, particularly in the vicinity of the explosion center, always yields lower values of the damage probabilities with respect to the probit models. Furthermore, it is clear from Table 5 that the use of vulnerability tables based on very low overpressure threshold values, as suggested by some other authors [17,18], may lead to extremely conservative results.

Even more important differences are present in the results reported in Table 5 for the pressure storage vessels (D101, D111, and D112). The probit model by Eisenberg et al. [15] is shown to yield the higher damage probabilities, above 0.5 in all but one case. Also the vulnerability model of Gledhill and Lines [17] yields high damage probabilities, although the overpressures on the D101 vessel are below the threshold of 38 kPa. On the other hand, the damage threshold of 70 kPa is never exceeded: no damage is expected on pressurized vessels using the approach of Khan and Abbasi. The probit model developed in the present study for pressure vessels yields low damage probabilities in all cases but one. Finally, the Bagster and Pitblado approach also yields low damage probabilities. In the following section it will be shown that these considerations will lead to important differences for the calculated risk indexes.

2.3. Case study 2: atmospheric tank farm and process vessels

Case study 2 again involves possible domino effects between atmospheric and pressurized storage vessels. However, important differences were present with respect to case 1: (i) the atmospheric tanks in this case contain fuels with higher volatility, thus requiring to take into account the UVCEs caused by pool vaporization as a consequence of accidental releases from the tanks; and (ii) a distillation column is present quite near the atmospheric storages, thus possible domino effects involving process vessels should be taken into account. A detailed list of the equipment and the distances between the equipment items considered in this analysis are shown in Tables 6 and 7. Fig. 5 shows the lay-out considered for the case study. Again, a simplified QRA of the case study was necessary to estimate the individual and societal risk indexes caused by primary accidental scenarios, not taking into account domino effect. Table 4 shows the primary scenarios used in the risk assessment. Figs. 6 and 7 show the individual and societal risk calculated in the absence of domino effect.

Table 6
Process and storage vessels considered in case study 2

Vessel	Type	Substance	Content, t
C615	Distillation column	N-hexane	5
TK80	Pressurized tank	Propane	50
D401	Atmospheric tank	Gasoline	2000
D402	Atmospheric tank	Gasoline	2000
D403	Atmospheric tank	Gasoline	2000
D404	Atmospheric tank	Gasoline	2000
D405	Atmospheric tank	Gasoline	2000
D406	Atmospheric tank	Gasoline	2000
D407	Atmospheric tank	Gasoline	2000
D408	Atmospheric tank	Gasoline	2000

Fig. 2 shows the overpressure curves with respect to the distance for the primary UVCEs that were considered as possible causes of domino effect. Table 8 reports the overpressures caused by the primary UVCEs on the equipment items considered in this case study.

Table 9 shows the damage probabilities calculated for the process and storage vessels considered in the analysis using three different approaches: (i) the probit models developed in part I [6]; (ii) the Bagster and Pitblado model [14]; and (iii) the vulnerability model proposed by Gledhill and Lines [17], based on a threshold value of 7 kPa for fixed roof tanks and of 38 kPa for pressurized tanks.

The limited inventory involved in the loss of containment from the distillation column C615 causes extremely low probabilities of triggering domino events by overpressure. On the other hand, Table 9 confirms the damage potential

Table 7
Distances (m) between storage and process vessels considered in case study 2

	C615	TK80	D401	D402	D403	D404	D405	D406	D407	D408
C615	–	253	85	130	179	124	163	200	165	190
TK80	253	–	188	137	85	203	158	115	223	182
D401	85	188	–	50	100	50	71	112	100	112
D402	130	137	50	–	50	71	50	71	112	100
D403	179	85	100	50	–	112	71	50	142	112
D404	124	203	50	71	112	–	50	100	50	71
D405	163	158	71	50	71	50	–	50	71	50
D406	200	115	112	71	50	100	50	–	112	71
D407	165	223	100	112	142	50	71	112	–	50
D408	190	182	112	100	112	71	50	71	50	–

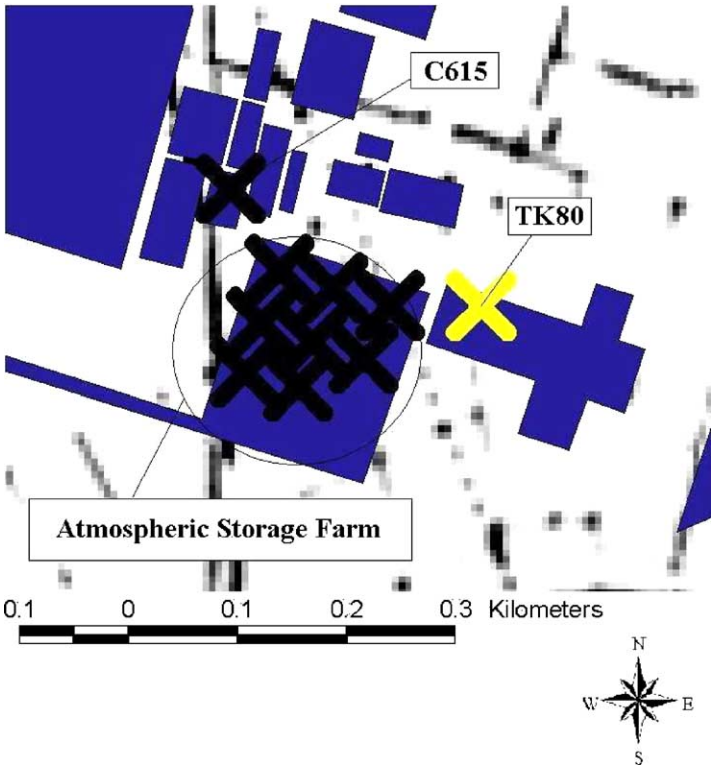

Fig. 5. Lay-out defined for case study 2.

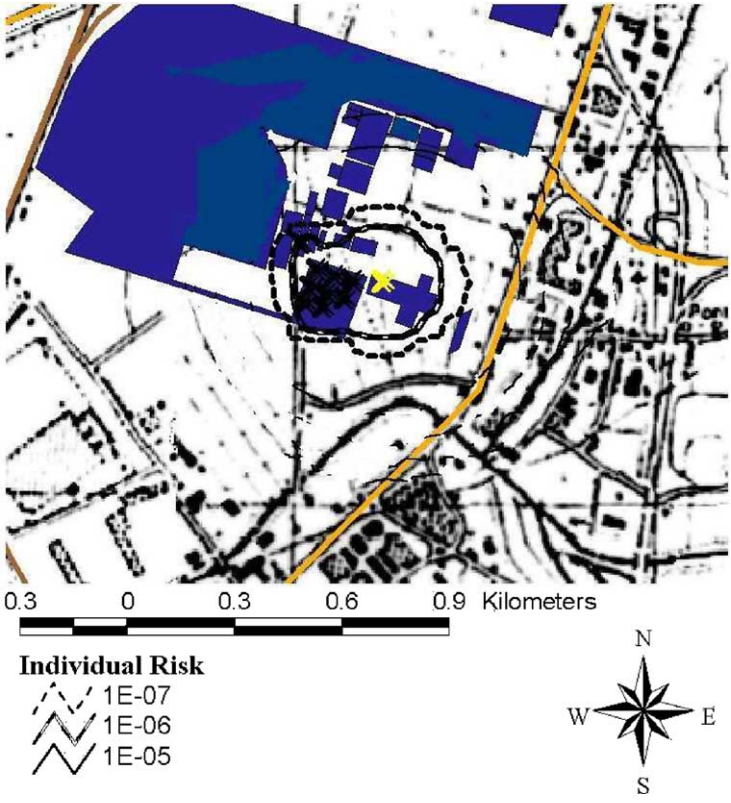

Fig. 6. Individual risk in the absence of domino effect for case study 2.

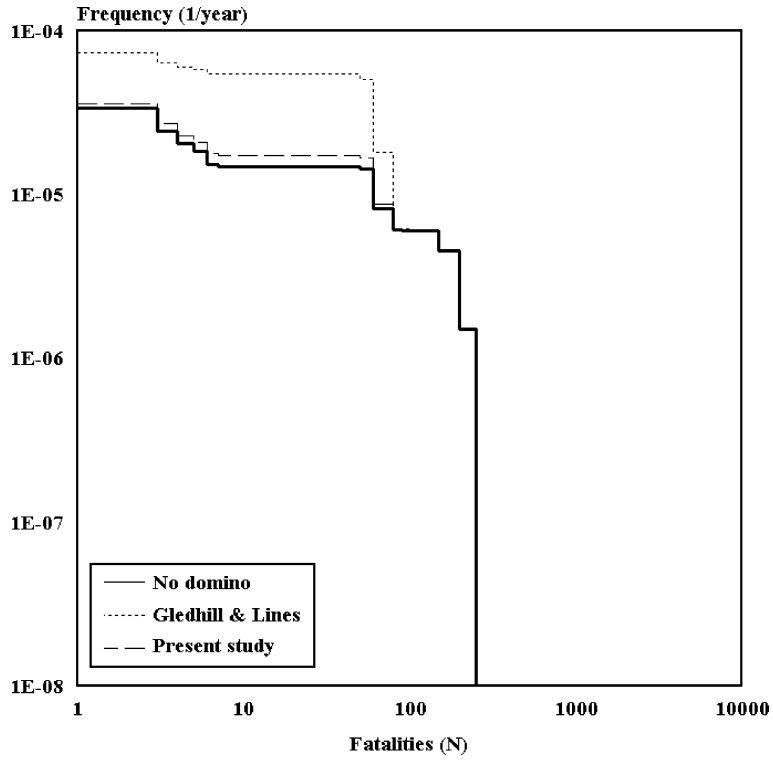

Fig. 7. Societal risk (*F–N* curves) calculated for case study 2.

of the severe UVCE considered for the TK80 pressure vessel. However, the main evidence that comes from this case study is that domino effects inside the tank farm originated from UVCEs, caused by the loss of containment of atmospheric vessels, are unlikely. Damage probabilities close to zero were found using the probit models developed, as well as the Bagster and Pitblado model. No damage ($F_d = 0$) is expected to be caused to nearby equipment by the UVCEs of atmospheric storage vessels (D401-D408) also in the approach proposed by Khan and Abbasi [16], since the 70 kPa threshold is never exceeded, as shown by Table 8. The damage probabilities obtained by the approach of Khan and Abbasi were very similar to those obtained with the Bagster and Pitblado approach, thus, were not reported in Table 9 for the sake of clarity.

As a matter of fact, the primary UVCEs considered for the atmospheric tanks resulted in very low overpressure (lower than 10 kPa) and consequently low effects on the nearby equipment. Although this result depends on the primary scenario and on the lay-out considered, it is well known that UVCEs having a high damage potential in the far field are not likely to be originated by the loss of containment of flammable liquids at ambient temperature. Nevertheless, completely different results could be obtained for the case study if a vulnerability threshold of 7 kPa, as suggested by some authors for fixed roof atmospheric storage tanks [17], was used. Table 9 shows the damage probabilities obtained by this approach.

The results obtained confirm that the selection of damage probability models is a key point in the quantitative assess-

Table 8
Peak overpressure (kPa) caused by primary UVCEs on process and storage vessels considered in case study 2

	C615	TK80	D401	D402	D403	D404	D405	D406	D407	D408
C615	–	19	5	2	1	3	1	0	1	0
TK80	0	–	0	2	5	0	1	3	0	0
D401	0	30	–	10	4	10	8	4	4	4
D402	0	55	10	–	10	8	10	8	4	4
D403	0	100	4	10	–	4	8	10	2	4
D404	0	28	10	8	4	–	10	4	10	8
D405	0	45	8	10	8	10	–	10	8	10
D406	0	81	4	8	10	4	10	–	4	8
D407	0	23	4	4	2	10	8	4	–	10
D408	0	29	4	4	4	8	10	8	10	–

Table 9
Damage probabilities calculated using different damage propagation models for case study 2

	C615	TK80	D401	D402	D403	D404	D405	D406	D407	D408
Present study										
C615	–	0.02	0.00	0.00	0.00	0.00	0.00	0.00	0.00	0.00
TK80	0.00	–	0.00	0.00	0.00	0.00	0.00	0.00	0.00	0.00
D401	0.00	0.88	–	0.07	0.00	0.07	0.03	0.00	0.00	0.00
D402	0.00	1.00	0.07	–	0.07	0.03	0.07	0.03	0.00	0.00
D403	0.00	1.00	0.00	0.07	–	0.00	0.03	0.07	0.00	0.00
D404	0.00	0.84	0.07	0.03	0.00	–	0.07	0.00	0.07	0.03
D405	0.00	0.99	0.03	0.07	0.03	0.07	–	0.07	0.03	0.07
D406	0.00	1.00	0.00	0.03	0.07	0.00	0.07	–	0.00	0.03
D407	0.00	0.73	0.00	0.00	0.00	0.07	0.03	0.00	–	0.07
D408	0.00	0.85	0.00	0.00	0.00	0.03	0.07	0.03	0.07	–
Bagster and Pitblado [14]										
C615	–	0.00	0.00	0.00	0.00	0.00	0.00	0.00	0.00	0.00
TK80	0.00	–	0.00	0.00	0.00	0.00	0.00	0.00	0.00	0.00
D401	0.00	0.00	–	0.00	0.00	0.00	0.00	0.00	0.00	0.00
D402	0.00	0.05	0.00	–	0.00	0.00	0.00	0.00	0.00	0.00
D403	0.00	0.26	0.00	0.00	–	0.00	0.00	0.00	0.00	0.00
D404	0.00	0.00	0.00	0.00	0.00	–	0.00	0.00	0.00	0.00
D405	0.00	0.01	0.00	0.00	0.00	0.00	–	0.00	0.00	0.00
D406	0.00	0.12	0.00	0.00	0.00	0.00	0.00	–	0.00	0.00
D407	0.00	0.00	0.00	0.00	0.00	0.00	0.00	0.00	–	0.00
D408	0.00	0.00	0.00	0.00	0.00	0.00	0.00	0.00	0.00	–
Gledhill and Lines [17]										
C615	–	1.00	0.00	0.00	0.00	0.00	0.00	0.00	0.00	0.00
TK80	0.00	–	0.00	0.00	0.00	0.00	0.00	0.00	0.00	0.00
D401	0.00	1.00	–	1.00	0.00	1.00	1.00	0.00	0.00	0.00
D402	0.00	1.00	1.00	–	1.00	1.00	1.00	1.00	0.00	0.00
D403	0.00	1.00	0.00	1.00	–	0.00	1.00	1.00	0.00	0.00
D404	0.00	1.00	1.00	1.00	0.00	–	1.00	0.00	1.00	1.00
D405	0.00	1.00	1.00	1.00	1.00	1.00	–	1.00	1.00	1.00
D406	0.00	1.00	0.00	1.00	1.00	0.00	1.00	–	0.00	1.00
D407	0.00	1.00	0.00	0.00	0.00	1.00	1.00	0.00	–	1.00
D408	0.00	1.00	0.00	0.00	0.00	1.00	1.00	1.00	1.00	–

ment of domino effect due to overpressure. In the following section, it will be shown that the use of very conservative approaches to damage probability may have an important effect also on the values of individual and societal risk.

3. The contribution of domino effect caused by overpressure to individual and societal risk

3.1. Individual and societal risk estimation in the presence of domino effect

The quantitative assessment of risk due to domino effect caused by overpressure required the definition of the secondary scenarios triggered by the loss of containment of secondary targets. Simplifying assumptions were necessary to afford calculations, and a limited number of representative secondary scenarios were defined.

In the case of atmospheric vessels, the more realistic hypothesis for the secondary scenario was considered a pool fire involving the entire vessel inventory. Indeed, the ignition can be considered as certain when explosion takes place, and extended damages are caused by the blast wave.

With respect to secondary events involving the LPG storage vessels, a wider number of scenarios are possible following the damage caused by overpressure. In particular, jet fires are expected if low intensity damages arise from the interaction with blast waves, while Fire balls are the most credible scenario following an extended damage of the vessels. Thus, two secondary scenarios were considered: a Fire ball, with a probability of 0.5, and a jet fire, with a probability of 0.5. Consequence evaluation of the secondary events was performed following the assumptions discussed for the primary events.

The methodology described in a previous study [8] was followed for the calculation of individual and societal risk due to the accidental scenarios caused by domino effects. In particular, the expected frequency of the secondary scenario was calculated by means of the following equation:

$$f_D = f_T F_s F_d F_e \quad (2)$$

where f_D is the resulting frequency of the domino event, f_T the expected frequency of the primary top event, F_s the

probability of the scenario causing the propagation, F_d the equipment damage probability, and F_e the probability of the secondary scenario given the failure of the target unit. The expected consequences were calculated from the vulnerability maps of the interacting scenarios:

$$V_D(x, y) = V_1(x, y) \cup V_2(x, y) \quad (3)$$

where V_1 and V_2 are the vulnerabilities (death probabilities) obtained from the probit functions for the primary and secondary scenarios at a generic location of co-ordinates (x, y) [13]. The approach proposed by Cozzani and Zanelli [8] was followed to define the probability combination in Eq. (2) and to calculate the vulnerability of domino events.

3.2. The contribution of domino caused by overpressure in case study 1

In order to understand the effect of domino events caused by overpressure, the individual and societal risk curves were calculated using the different damage probability models which were previously described. The results obtained using the probability models developed in the present study, reported in Fig. 8. Fig. 9, shows the individual risk curves obtained if the domino contribution is calculated using the probit model given by Eisenberg et al. [15]. Fig. 4 reports the calculated *F–N* societal risk curves. The figure also reports, for the sake of comparison, the *F–N* curves obtained using the Bagster and Pitblado model [14], and the vulnerability model based on the threshold values proposed by Gledhill and Lines [17]. The *F–N* curve obtained with the approach proposed by Khan and Abbasi [16] resulted in a curve completely overlapped to the *F–N* curve obtained in the absence of domino effect and was not reported in the figure.

In order to assess the maximum uncertainty that may be introduced by the use of different damage probability models in the present approach, individual and societal risk were also calculated considering the damage probability always equal to 1 for all the units. The results obtained for individual risk are reported in Fig. 10, and those for societal risk are shown in Fig. 4.

The comparison of Figs. 3 and 8–10 shows that both the 10^{-7} and the 10^{-6} per year isorisk curves cover wider areas as domino effect is introduced. As expected, the area inside the 10^{-7} per year isorisk curve progressively extends as the domino probabilities are calculated with the probit models developed in the present study and with the probit developed by Eisenberg et al. [15]. An even wider area is obviously obtained if the damage probability is assumed equal to one (damage is sure), as shown in Fig. 10.

Coming to the results obtained for societal risk, Fig. 4 shows that limited differences are present in the *F–N* curves for fatalities lower than 100. This region of the *F–N* curve is mainly influenced by the consequences of primary Pool fires of atmospheric storage tanks D401–D411. Even if wide

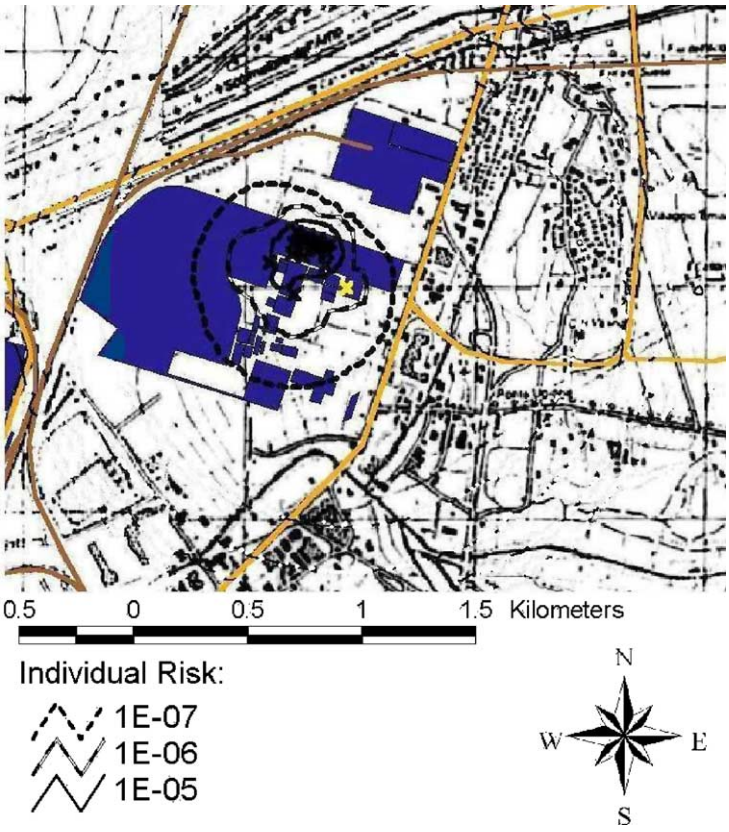

Fig. 8. Individual risk in case study 1 taking into account domino effect due to overpressure using the probit models developed in the present study.

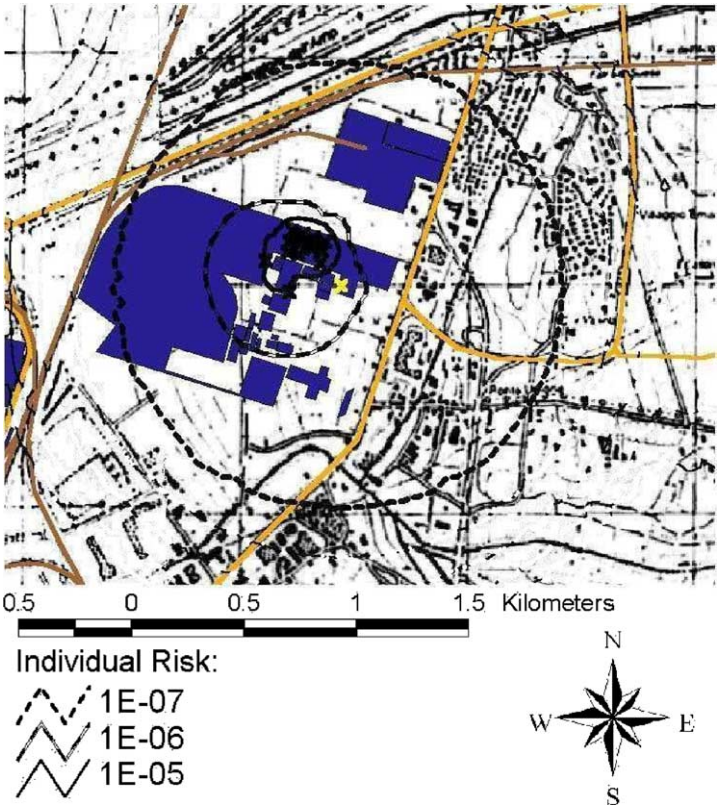

Fig. 9. Individual risk in case study 1 taking into account domino effect due to overpressure using the probit model proposed by Eisenberg et al. [15].

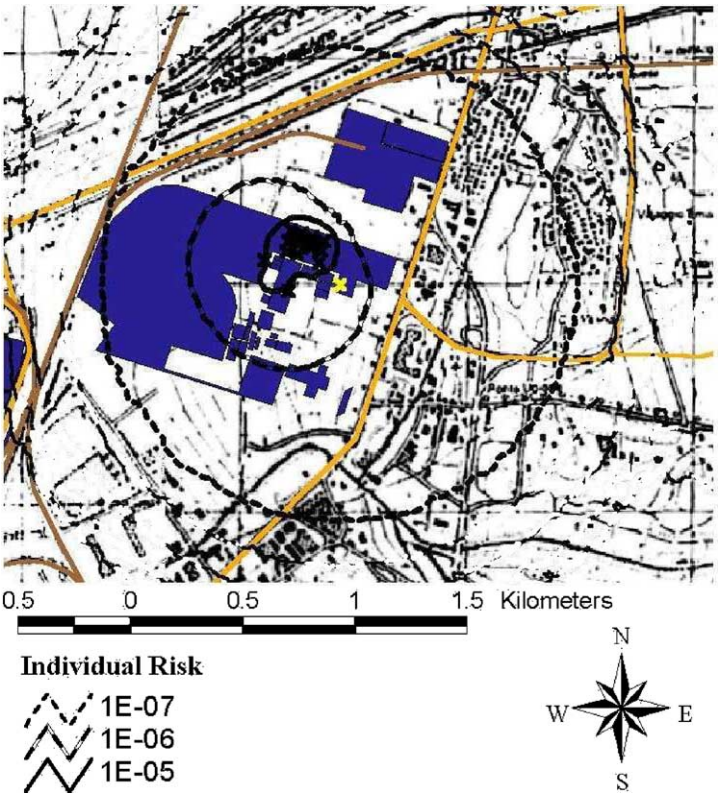

Fig. 10. Individual risk in case study 1 taking into account domino effect due to overpressure, considering a unit value of damage probability for all the process equipment.

damages are expected in the atmospheric storage park, low effects result on societal risk, since the primary accident frequencies considered for these vessels are about an order of magnitude higher than frequencies of domino events, as shown in Table 3.

The maximum number of fatalities in the *F–N* curves is almost the same in the presence and in the absence of domino effect. This result is specific for this case study, since the increase in the number of fatalities caused by secondary UVCEs is limited in the presence of low population densities. On the other hand, Fig. 4 shows that the influence of domino effects on the *F–N* curve is mainly in the 100–1000 fatalities region. In this zone, the wide differences between the approaches depend on the different damage probability values obtained for the pressurized vessels D101, D111 and D112. In the same region of the curve, as expected, assuming damage probability always equal to one ($F_d = 1$, damage is certain) results in the maximum societal risk value, corresponding to an increase of about one order of magnitude. The Eisenberg probit model [15] results in lower values of societal risk. However, this model yields the highest societal risk values with respect to all the other damage probability models considered in this case study. The vulnerability approach proposed by Gledhill and Lines [17] leads to slightly lower frequency values. The approach developed in the present study yields risk values that are intermediate between those obtained in the absence of domino effect and those obtained from the use of the probit model by Eisemberg et al. [15]. On the other hand, the approaches of Bagster and Pitblado [14] and of Khan and Abbasi [16] lead to results that are almost coincident with those obtained in the absence of domino effect. These results are confirmed if the "expectation value" (EV) or potential life loss is calculated from the *F–N* curves. The results are reported in Table 10. The table shows that, in case study 1, only a limited increase of the EV is present (about 50% in the worst case), even if a unit propagation probability is considered ($F_d = 1$). The results also confirm that the use of the Khan and Abbasi model and the Bagster and Pitblado model leads to the estimation of a very low contribution of domino effect caused by overpressure to societal risk. On the other hand, the comparison of the results obtained with the Eisenberg approach and with the probit functions developed in the present study shows that the introduction of equipment specific probit functions causes 10% decrease in EV, although the increase of risk due to domino effect is still appreciable (about 10% with respect to the absence of domino effect). Therefore, the results obtained confirm that the use of specific damage probability models for different equipment categories is crucial in the quantitative assessment of domino effect due to overpressure.

3.3. The contribution of domino caused by overpressure in case study 2

The lower damage probabilities in case study 2 result in lower increases of the values of individual and societal risk due to domino effect. Fig. 11 reports the individual curves obtained using the probit models developed herein, while Fig. 12 shows the isorisk curves obtained using damage probabilities derived from the vulnerability model of Gledhill and Lines [17]. The comparison with the results obtained in the absence of domino effects, shown in Fig. 6, evidences that using either of the damage probability models leads to an increase of the area inside the 10^{-6} and 10^{-7} per year isorisk. However, the contribution of domino events to individual risk is lower than that in case study 1. Furthermore, the comparison of Figs. 11 and 12 points out that the Gledhill and Lines [17] vulnerability model yields to higher risk figures with respect to those obtained using the equipment-specific probit functions.

Fig. 7 reports the *F–N* curves obtained from societal risk calculations for all the damage probability models. In this case study, the main differences in the societal risk *F–N* curve arise in the region between 0 and 60 fatalities. This region is mainly influenced by the risk related to the atmospheric storage vessels. Indeed, Fig. 2 shows that the UVCEs from the atmospheric storage vessels have a much lower damage range than UVCEs originated by LPG vessel failure. However, the higher frequencies that should be attributed to these events (see Table 3 [11]) result in domino frequencies of the same order of magnitude of the primary events. This causes a moderate increase of the frequency values in the *F–N* curve, although the small damage range of secondary accidents limits the severity of the domino events. Fig. 7 also evidences that the increase in the frequency values of

Table 10
Expectation values resulting for the two case studies using different damage probability models

Damage probability model	Case 1		Case 2	
	EV, fatalities per year	Increase (%)	EV, fatalities per year	Increase (%)
No domino	7.88×10^{-3}	–	1.86×10^{-3}	–
$F_d = 1$	11.90×10^{-3}	51.1	n.a.	n.a.
Gledhill and Lines [17]	10.64×10^{-3}	35.0	4.40×10^{-3}	137.0
Eisenberg et al. [15]	9.80×10^{-3}	24.4	n.a.	n.a.
Present study	8.68×10^{-3}	10.2	2.02×10^{-3}	8.7
Khan and Abbasi [16]	8.34×10^{-3}	5.8	1.86×10^{-3}	0.4
Bagster and Pitblado [14]	7.97×10^{-3}	1.2	1.91×10^{-3}	3.0

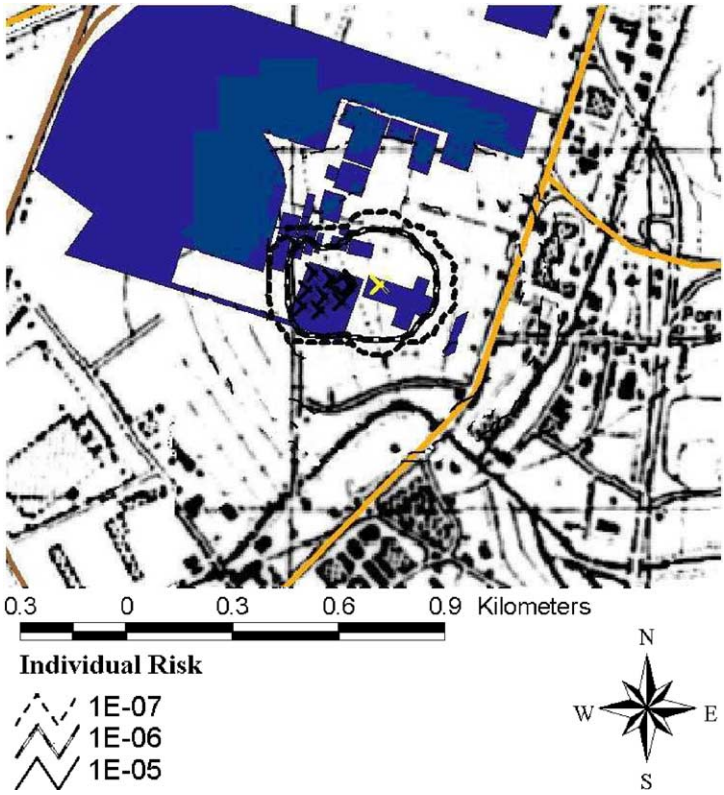

Fig. 11. Individual risk in case study 2 taking into account domino effect due to overpressure using the probit models developed in the present study.

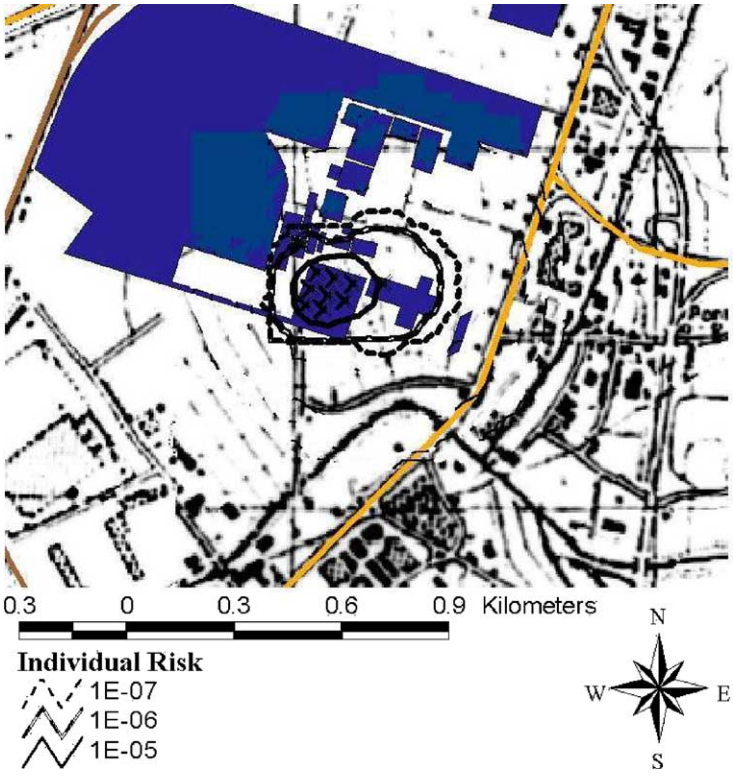

Fig. 12. Individual risk in case study 2 taking into account domino effect due to overpressure using the vulnerability model of Gledhill and Lines [17].

the societal risk *F–N* curve is always lower than a factor of two in this case study. As expected, the Gledhill and Lines [17] approach is very conservative and yields the highest *F–N* curve. On the other hand, the *F–N* curves obtained from the models of Bagster and Pitblado [14] and Khan and Abbasi [16] resulted almost coincidenting with the *F–N* curve obtained, if not considering the domino effect, and were not reported in the figure. These results are confirmed by the calculated expectation values, reported in Table 10. The EV is almost coincidenting in the absence of domino effect or considering domino effect using the damage probability models of Bagster and Pitblado [14] and Khan and Abbasi [16]. Again, these approaches lead to very low increases of the individual and societal risk due to domino effect caused by overpressure. Thus, also case study 2 confirms the importance of the models selected for the assessment of damage probability.

4. Conclusions

Two case studies were performed in order to obtain a quantitative assessment of the contribution to industrial risk of domino effect caused by overpressure. Different damage probability models were applied to estimate domino frequencies. A first important result of the study is that, a straightforward estimation of the main risk indexes taking into account of domino effect is possible using the approach proposed. The results also pointed out that domino effects caused by overpressure may have important effects on societal and individual risk. An increase of societal risk up to an order of magnitude is possible, depending on the damage probability model used and on the characteristics of the site.

The specific probit models developed in part I for the assessment of equipment damage probability can be used for a quantitative assessment of domino hazard contribution to industrial risk with a limited calculation effort.

The comparison with other proposed approaches showed that the probit models developed permit to take easily into account the equipment characteristics, limiting the problems due to the possibility of over conservative estimates that may derive from the use of vulnerability tables or threshold values. On the other hand, the probit models resulted sufficiently sensitive to appreciate the risk increase due to overpressure domino effect. Hence, the results of the case studies confirmed that the use of specific damage models for the different equipment categories is necessary for a reliable quantitative assessment of the contribution of domino effect caused by overpressure to individual and societal risk indexes.

References

[1] F.P. Lees, Loss Prevention in the Process Industries, second ed., Butterworth–Heinemann, Oxford, UK, 1996.
[2] K. Rasmussen, The experience with the major accident reporting system from 1984 to 1993, EUR 16341 EN, Commission of the European Communities, Luxembourg, 1996.
[3] CCPS, Guidelines for Chemical Process Quantitative Risk Analysis, second ed., AIChE, New York, 2000.
[4] G.N. Pettitt, R.R. Schumacher, L.A. Seeley, J. Loss Prev. Process Ind. 6 (1993) 37.
[5] S. Contini, S. Boy, M. Atkinson, N. Labath, M. Banca, J.P. Nordvik, Proceedings of European Seminar on Domino Effects, Leuven, 1996, p. 1.
[6] V. Cozzani, E. Salzano, The quantitative assessment of domino effects caused by overpressure. Part I. Probit Models, J. Hazard. Mater. 107 (2004) 67.
[7] G. Spadoni, D. Egidi, S. Contini, J. Hazard. Mater. 71 (2000) 423.
[8] V. Cozzani, S. Zanelli, Proceedings of 10th International. Symposium. on Loss Prevention and Safety Promotion in the Process Industries, Elsevier, Amsterdam, 2001, p. 1263.
[9] C. Delvosalle, Proceedings of European Seminar on Domino Effects, Leuven, 1996, p. 11.
[10] S.P. Kourniotis, C.T. Kiranoudis, N.C. Markatos, J. Hazard. Mater. 71 (2000) 239–252.
[11] P.A.M. Uijt de Haag, B.J.M. Ale, Guidelines for Quantitative Risk Assessment (Purple Book), Committee for the Prevention of Disasters, The Hague, NL, 1999.
[12] C.J.H. Van Den Bosh, R.A.P.M. Weterings, Methods for the Calculation of Physical Effects (Yellow Book), Committee for the Prevention of Disasters, The Hague, NL, 1997.
[13] D. Egidi, F.P. Foraboschi, G. Spadoni, A. Amendola, Reliabil. Eng. Syst. Safety 49 (1995) 75.
[14] D.F. Bagster, R.M. Pitblado, Process Safety Environ. Protect. 69 (1991) 196.
[15] N.A. Eisenberg, C.J. Lynch, R.J. Breeding, Vulnerability Model: A Simulation System for Assessing Damage Resulting from Marine Spills, Report CG-D-136-75, Enviro Control Inc., Rockville, MD, 1975.
[16] F.I. Khan, S.A. Abbasi, Process Safety Progr. 17 (1998) 107.
[17] J. Gledhill, I. Lines, Development of Methods to Assess the Significance of Domino Effects From Major Hazard Sites, CR Report 183, Health and Safety Executive, 1998.
[18] G. Ballocco, A. Carpignano, G. Di Figlia, J.P. Nordvik, L. Rizzuti, Proceedings of European Conference on Safety and Reliability, ESREL, Torino, 2001, p. 2029.
[19] I.L. Hirst, D.A. Carter, J. Hazard. Mater. 92 (2002) 223.